

SOFTWARE APPLICATION TO INVESTIGATE COINCIDENCES OF THE MUONIC RADIATION WHEN PASSING THROUGH THE MULTI PIXEL PHOTON COUNTER (MPPC) UNDERGROUND DETECTOR

L. NIȚĂ

University of Bucharest, Faculty of Physics, Doctoral School of Physics, Romania
E-mail: nitaliviu@outlook.com

Received July 18, 2022

Abstract. This software application can be successfully used in a quick calculation of the spatial distribution of muonic radiation passing through the detector. The software provides multiple sets of already processed data for various graphical representations.

Key words: software, muon, underground, SiPM detectors, MPPC detectors, databases, online.

1. INTRODUCTION

The exponential development of the IT technique of the recent times allows the simulation of a growing number of phenomena in physics and especially in nuclear and astrophysical physics. Thus, it is normal to look for new numerical relations, even if it does not differ in its mathematical significance.

The need for data processing in real time, the elimination of trajectories that do not coincide and therefore only agglomerate the graph by appropriate numerical methods make this application and, many more that can be written as a base – lead to various automation or data display methods. Thereby it can be extended the field of applicability more than the ones listed above.

This article shows explicitly the main routines of the software, meaning the primary processing of the raw data provided by the receiver module connected to the detector. The online routine giving the results cannot be shown here considering the space given. The functions of the software can be applied in various scientific fields such as: mapping cavities for non-destructive study and exploration of the archaeological sites, caves, salt or coal mines, testing the homogeneity of the slopes of hydrotechnical dams, examination of the dam's structure, a real time observation of the shipping crossing some specific points such as terrestrial or water customs barriers.

This article describes the main routines underlying the application calibration for two detector geometries. The data thus obtained are used to compose the most representative graphs from which the quality and the amount of the muon flow can be deduced.

2. MEASURING MUON FLUX IN THE IFIN-HH LABORATORY INSIDE THE SALT MINE OF SLĂNIC PRAHOVA

2.1. THE “UNIREA” MINE LOCATED IN SLĂNIC, PRAHOVA DISTRICT

Since 2004, the “Unirea” mine in Slănic Prahova hosts a laboratory for IFIN-HH, built to carry out measurement of high energy cosmic radiation. The main reason this location was chosen is that it has an exceptionally low levels of background radiation, which is key in the performing accurate measurements of muons and neutrons.

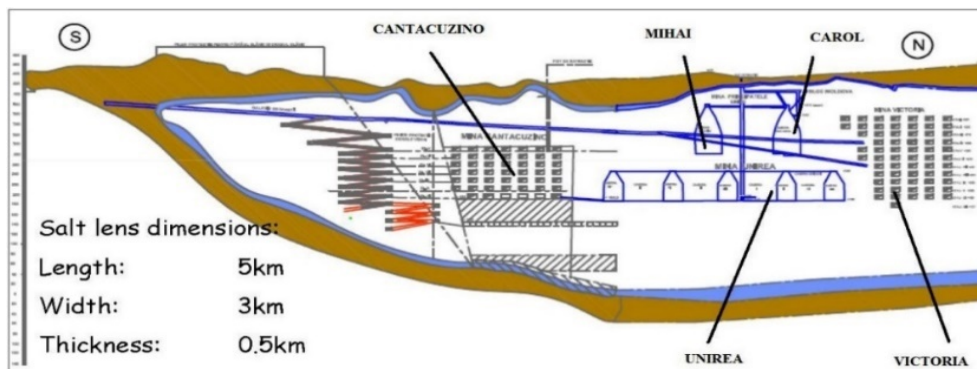


Fig. 1 – Cross-section of Slănic Prahova mine complex.

“Unirea” mine, located at a depth of 208 m, is made up of 14 trapezoidal rooms with 10 m opening to the roof, and from 32 m to 36 m opening to the base. The mine has a height of approximately 55 m. Mean measurements for the mine are as follows: temperature: 12°C, humidity: 65–70%, atmospheric pressure: 730 mm of mercury.

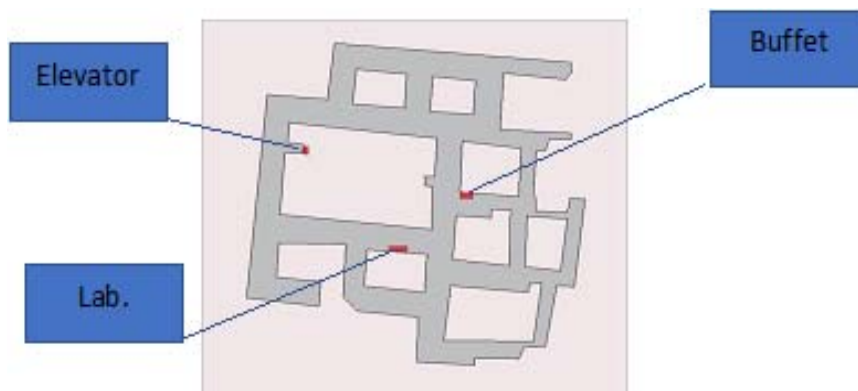


Fig. 2 – Location plan of IFIN-HH laboratory.

2.2. UNDERGROUND DETECTOR WITH PLASTIC SCINTILLATORS AND MPPC (MULTI PIXEL PHOTON COUNTER) PHOTODIODES, USED BY IFIN-HH

The plastic scintillator detector works because charged particles interact with the scintillator, thereby releasing energy in its material. This scintillation is taken by wavelength and the light signal is then transported to the photomultiplier where it is converted into an electric signal.

The detector uses SiMP diodes, unlike the older generation which used photomultipliers to transform the light signal into an electrical impulse. Similarly, to the older technology, the cosmic radiation particles interact with the detector's scintillator, therefore the scintillation due to the energy left by the particles is produced. The scintillation is captured but the fiber optic, and the photons are transformed into an electric signal with the help of the MPPC photodiodes who act as a photomultiplier. Further on, the electric signal is transformed into a logic signal with the help of the discriminator [1].

Multi Pixel Photon Counter (MPPC) is a device that transforms the light signal into an electric signal proportional to the number of incident photons. It is made up of diodes connected in series together with resistors for attenuation. It belongs to the SiPM (Silizium-Photomultiplier) device category, semiconductors based on light detectors, which in comparison with classic photomultipliers, has the following advantages for particle detection devices:

- lower voltage power supply (70...72 V) than photomultipliers (2 kV);
- higher detection density due to the photodiodes' converters being significantly smaller than photomultipliers' converters;
- higher photon detection probability;
- improved temporal resolution;
- very high efficiency in reconstruction of the muon trajectories.

The muon detector used by IFIN-HH in the Slănic Prahova salt mine is designed to have three detection planes, each made up of two detectors which determine the position (x and y coordinates) at which the muon radiation has entered and exited the detection area [2].

The system as a whole is able to determine the angle of incidence of the trajectory of the muon entering the system. This enables us to specify the muon radiation density with respect to the cartesian or spherical coordinates whose origin is the center of the detection system [3].

In other words, where we see more muons coming in and where we see less muons coming in. We can say with precision, due to the attenuation of the radiation flux when passing through blocks of material with different densities, if beyond the rock wall there are cavities or not.

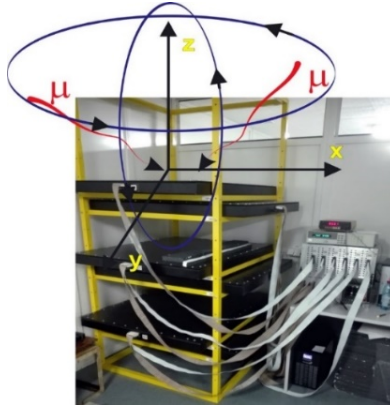


Fig. 3 – The detection system.

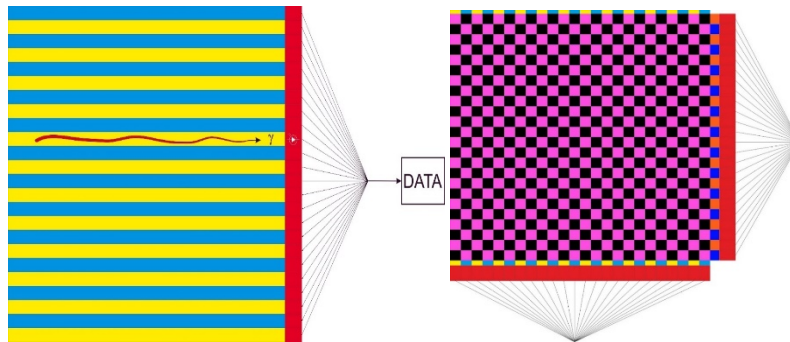


Fig. 4 – Schematic of the acquisition surface.

The design dimensions of the detection system are as follows:

- the surface of a detection with scintillation is $(0.04 \text{ m}) \times (1 \text{ m})$;
- distance between the two x/y detector planes is 0.14 m.

Distance between the three detection planes can be changed as needed. The time base used is measured and maintained with a precision of a thousandth of a second.

To be able to also determine the y coordinate of the position at which the muon entered the system, the same type of detector is placed in close proximity, but with the waveguides perpendicular to the other detector.

This detector has plates with scintillators on which 24 waveguides are mounted, which then transmit the photons approximately 1 m away to the photodiode. The photodiode sends the electric signal to a data acquisition board. This data module, connected to the detector with 6 connectors, has a suggestive interface (Fig. 5) showing the events in real time.

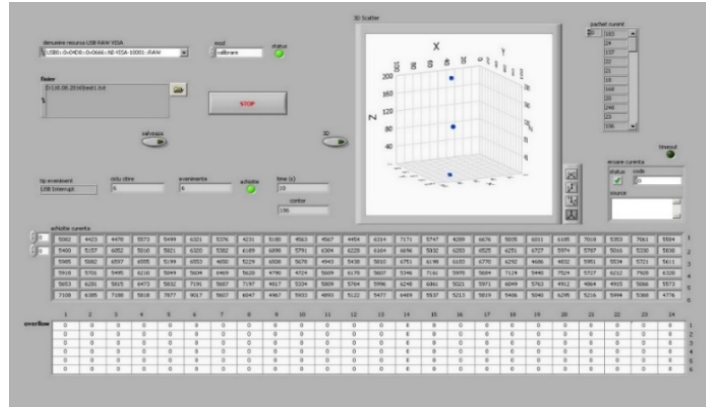


Fig. 5 – Data module interface.

The data set subject to processing with this custom-built application, has the following acquisition parameters:

- 10.08.2016 1:40PM start air conditioning 25 degrees; 7.51 V main;
- 11.08.2016 11:14AM stop 1661829e – 77625.8 s;
- total number of events registered = 1 661 829 during approximately 21.5 hours;
- the distance between the three detection planes is 0.51 cm.

The data collected from the acquisition board during the time period indicated above are in text format.

In a first, suggestive description we have for the time stamp in the first column, the corresponding hits or not, indicated by 1 and 0 respectively, of the scintillator cell detecting the position (x, y) for each to the 3 planes (Fig. 6).

time	ax1	ax2	ax3	ax4	ax22	ax23	ax24	ay1	ay2	ay3	ay4	cy20	cy21	cy22	cy23	cy24
0.011	0	0	0	0	0	0	0	0	0	0	0	0	0	0	0	0
0.024	0	0	0	0	0	1	0	0	0	0	0	0	0	0	0	0
0.026	0	0	0	0	0	0	0	0	0	0	0	0	0	0	0	0
0.109	0	0	0	0	0	0	0	0	0	1	0	0	0	0	0	0
39.96	0	1	0	0	0	0	0	0	0	0	0	0	0	0	0	0
39.982	1	0	0	0	0	0	0	0	0	0	0	0	1	0	1	1
39.997	0	0	0	0	0	0	0	0	0	0	0	0	0	1	0	0
40.003	0	0	1	0	0	0	0	0	0	0	1	0	0	1	0	0
40.037	0	0	0	1	0	0	0	0	0	0	0	1	0	0	0	0
40.079	0	0	0	0	0	0	0	0	0	0	1	0	0	0	0	0
40.111	0	0	0	0	0	0	0	0	0	0	0	0	0	0	0	0
40.155	0	0	0	0	0	0	0	0	0	0	0	0	0	0	0	0
40.183	0	0	0	0	0	0	0	0	0	0	0	0	0	0	0	0
40.187	0	0	0	0	0	0	1	0	0	0	0	0	0	0	0	0
40.197	0	0	0	0	0	0	0	0	0	0	0	0	0	0	0	0
40.231	0	0	0	0	0	0	0	0	0	0	0	1	0	0	0	0
40.246	0	0	0	0	0	0	0	0	0	0	0	0	0	0	0	0
40.339	0	0	0	0	0	0	0	0	0	0	0	0	0	0	0	0

Fig. 6 – The text format of the data output.

2.3. DESCRIPTION OF THE APPLICATION SPECIALLY CREATED FOR THIS PURPOSE

This application can be used successfully to calculate, quickly, the spatial distribution of muonic radiation as it passes through the detector. The application

provides multiple data sets already processed and ready for various graphical representations, as shown further down.

It should be mentioned that it is easy to configure, *via* an online interface, numerous geometries of this detector which can be used in different modes.

The data packets obtained for various measurement purposes are easily inputted in the application database for processing, allowing for their storage to be indexed so a history of the data can be generated. A feature of the application is that it allows you access to the stored data online, by assigning certain rights, accessed with a user and password.

As well as the online data input and processing, the application can also be used successfully for real-time data processing if, for example, the detector is set up for immediate processing.

Before starting data analysis, information about the study process must be entered into the application, accessed by user login as shown in the images above.

After the configuration characteristics for the identification of the study process have been entered in the data base, data which should also include information about detector geometry, meaning the distance between the detection planes and also the error that will apply to the data set, the import of the file generated by the detector can begin.

As it is natural also to introduce the code by which the selection of the coincidence vectors is done, I'll also describe parameters and object names which appear in the code, either through suggestive images or through descriptive text.

To transfer the processed data to the online medium I used the following command:

```
! psftp.exe *****@*****.*** -pw *****. -b ssh.txt
```

where the ssh.txt file contains the code below.

```
put transfer.txt
** for full code please visit web https://liviunita.ro/download/full\_article.docx.zip
put semafor.txt
```

As shown, at the very last the semafor.txt file is loaded in which signals to the database that the transfer has finished, and that the data can be imported in the tables predetermined and defined in database.

The Linux server will know it can load the already transferred data into the online tables through the execution of a file with the structure shown below, in the service of Scheduled Cron Jobs.

The semafor.sh file

```
clear
** for full code please visit web https://liviunita.ro/download/full\_article.docx.zip
fi
```

To start with, the detection identification data are uploaded, as well as the geometry, as shown in Fig. 7.

Denumire	Data	Observatii	Finalizat	Numar Coincidente
(+/-)0.080m Slanic Prahova (21.5 ore de receptie 15.11.2017 bis3	22.07.2020	10.08.2016 1:40PM start aer conditionat 25 grade; 7.51V main; - 11.08.2016...	✓	18 859 760

Actiuni	Distanța dintre cele 3 plane (metri)	Eroare de masurare (metri)	Observatii
	0.520	0.080	NULL

Fig. 7 – The loading of the detection identification data.

Once these have been entered, the application can identify in the database the process that needs to be analyzed and will ask for the data recorded by the detector. After initializing the general entry data and preparing the databases according to the code below it will ask to locate the file containing the detection data [4].

CLOSE DATABASES

** for full code please visit web https://liviunita.ro/download/full_article.docx.zip
Endif

After the primary data have been brought into the application, the constants of the detection that will be processed according to the algorithm described further on are displayed.

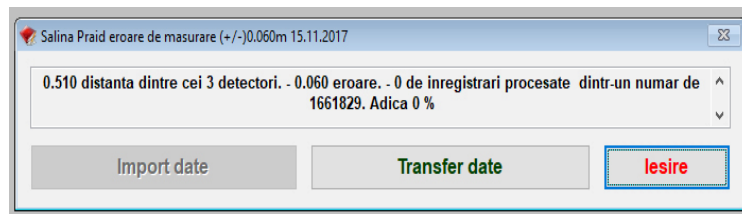


Fig. 8 – Processing constants displayed before the transfer to the database.

The application separates the $x_1, y_1, x_2, y_2, x_3, y_3$ trajectory coordinates of the muonic radiation through the three detection planes of the detector, then runs the extraction of the particles which give coincidences in the three planes (A, B, C), described in figure below, from the total incident particles, according to the formula of 3 collinear points in the three-dimensional space [5]

$$\frac{x_3 - x_1}{x_2 - x_1} = \frac{y_3 - y_1}{y_2 - y_1} = \frac{z_3 - z_1}{z_2 - z_1}. \quad (1)$$

By solving the system, we get the following relationships:

$$x_3 = \frac{z_3 - z_1}{z_2 - z_1}(x_2 - x_1) + x_1 \quad (2)$$

$$y_3 = \frac{z_3 - z_1}{z_2 - z_1}(y_2 - y_1) + y_1. \quad (3)$$

According to Fig. 9, the maximum value for the error caused by the dimensions of the detection cell with a value of 0.04 m (the detector cell is a square with a side of 0.04 m) is of (+/-) 0.06 m.

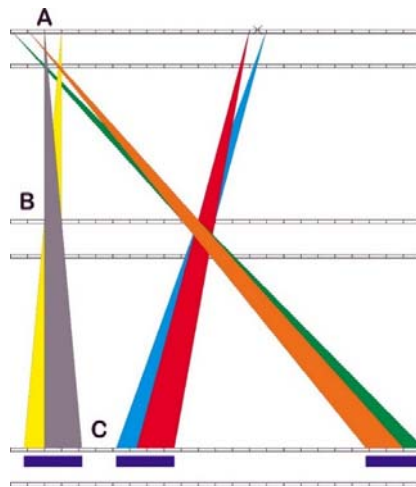


Fig. 9 – The muon trajectories incidence with the three detection planes.

Which is translated into the following relationships, if we consider that we have a measuring uncertainty for x and y equal to the variable $_e_x3$ and $_e_y3$, we then have in the application the collinearity condition shown below.

WHERE X3.x3 BETWEEN
 $(X1.x1 + ((X2.x2 - X1.x1) * ((_z3) - (_z1))) / ((_z2) - (_z1))) - (_e_x3)$ AND $(X1.x1 + ((X2.x2 - X1.x1) * ((_z3) - (_z1))) / ((_z2) - (_z1))) + (_e_x3);$
 AND Y3.y3 BETWEEN
 $(Y1.y1 + ((Y2.y2 - Y1.y1) * ((_z3) - (_z1))) / ((_z2) - (_z1))) - (_e_y3)$ AND $(Y1.y1 + ((Y2.y2 - Y1.y1) * ((_z3) - (_z1))) / ((_z2) - (_z1))) + (_e_y3);$

The primary routine of the application is posted below. Each row in the imported data table is treated separately, checking to see if the spatial collinearity equations described above are respected [6].

```
SELECT dat
** for full code please visit web https://liviunita.ro/download/full_article.docx.zip
ENDIF
```

From this program sequence we observe the extraction of the coordinates (x_3, y_3) for the coincidence through the exit plane of each point (x_1, y_1) from the entry plane, if the incidence condition is satisfied [7].

Also extracted are the value of the size of vector r , and of the theta and phi angles in radians, necessary in a spherical representation.

They are all loaded in several tables (transfer.txt, analiza.txt, count_iesire.txt, count_intrare.txt, phi.txt, theta.txt) which at the end are sent through a ssh channel to the online database.

For the complete option (“full-time, online”), this application runs while permanently connected to the detector data module. It constantly transmits, in real time, the processed data, meaning it extracts the coincidences and calculates the cartesian and spherical coordinates of the vectors. The results are sent into a database which can be accessed online. By accessing them securely through a user and password, the desired results can be selectively extracted.

The data used in the build and calibration of the application were obtained by courtesy of Professor Bogdan Mitrică from the Horia Hulubei National Institute for R&D in Physics and Nuclear Engineering (IFIN-HH). The detection took place are IFIN-HH in the Slănic Prahova salt mine.

The general data used for all approximations in calculations are:

- the side of the detector (in the shape of a square) is 0.04 m;
- the equal distance between the three planes of detection is of 0.51.

For the initial data set, containing 1 661 830 counts taken over 21.5 hours, several variants of approximating the graph were chosen.

Table 1

Calculation options for establishing the maximum number of coincidences

Approximation	Number of Coincidences
(+/-) 0.000 m	947 180
(+/-) 0.020 m	947 180
(+/-) 0.040 m	7 392 577
(+/-) 0.060 m	7 392 577
(+/-) 0.070 m	7 392 577
(+/-) 0.075 m	7 392 577
(+/-) 0.080 m	18 859 760
(+/-) 0.120 m	22 524 794

From the graphical representation above (which is drawn to scale, Fig. 9), it can be observed that the correct maximum coincidences possible is calculated in the range [(+/-) 0.040 m, (+/-) 0.080 m]. Beyond this error the coincidences' number rises suddenly, by a lot and falsely, and under (+/-) 0.040 m it is possible we are not considering all possibilities. The results of these calculations are shown in the following graphs.

We'll consider, for comparative representation, three of the statistics mentioned above, that is the measurements corresponding to $(\pm) 0.040$ m and $(\pm) 0.080$ m.

The online application supplies in real-time a graph for each statistic, as shown in the images below.

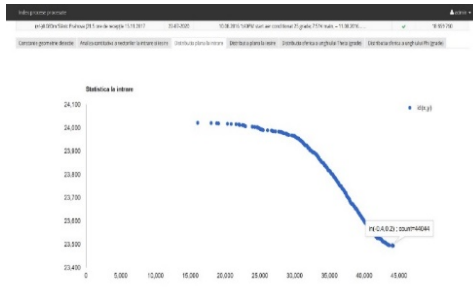


Fig. 10 – Flat distribution at entry.

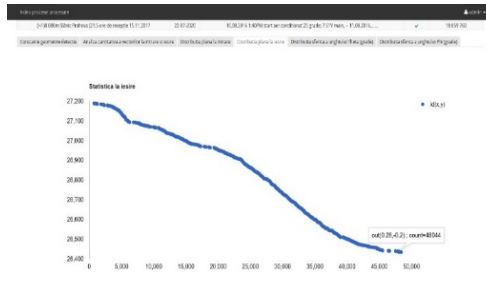


Fig. 11 – Flat distribution at exit.

3. RESULTS OF MEASURING MUON FLUX IN THE IFIN-HH LABORATORY INSIDE THE SALT MINE OF SLĂNIC PRAHOVA

3.1. MUONIC COINCIDENCE DISTRIBUTION WHEN ENTERING THE DETECTOR

For the statistical entry (the “Flat distribution at entry” menu of the online application), the following code was used [8].

```
SELECT Datfin.cuprins, Datfin.x1, Datfin.y1, COUNT(Datfin.cuprins);
FROM fit!datfin GROUP BY Datfin.cuprins, Datfin.x1, Datfin.y1 ORDER BY 4 DESC
```

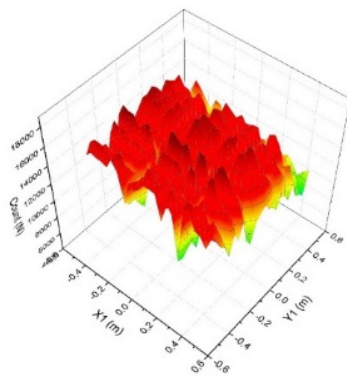


Fig. 12 – Statistical entry – for a measuring uncertainty of $(\pm) 0.04$ m.

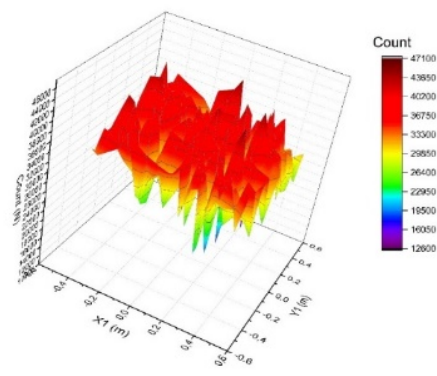


Fig. 13 – Statistical entry – for a measuring uncertainty of $(\pm) 0.08$ m.

```
SELECT Datfin.cuprins, Datfin.x3, Datfin.y3, COUNT(Datfin.cuprins);
FROM fit!datfin GROUP BY Datfin.cuprins, Datfin.x3, Datfin.y3 ORDER BY 4 DESC
```

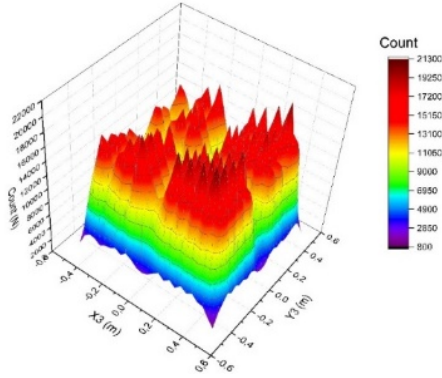


Fig. 14 – Statistical entry – for a measuring uncertainty of (+/-) 0.04 m.

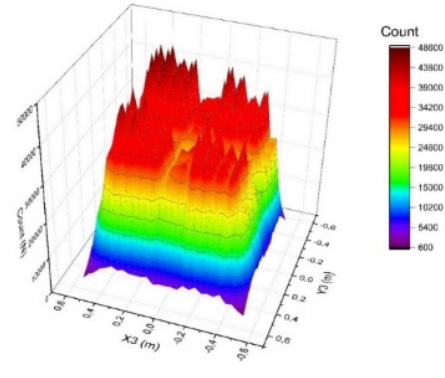


Fig. 15 – Statistical entry – for a measuring uncertainty of (+/-) 0.8 m.

3.2. THREE-DIMENSIONAL DISTRIBUTION OF MUONIC RADIATION COINCIDENCE THROUGH THE DETECTOR

For the statistical vector the following code was used

**code for cart2dec*

```
SELECT DISTINCT Datfin.x1, Datfin.y1, Datfin.z1, Datfin.x3, Datfin.y3, Datfin.z3,;
** for full code please visit web https://liviunita.ro/download/full\_article.docx.zip
```

Table 2

(Truncated) table containing data for the statistical analysis of incident vectors with approximation of 0.04 m

Nr. Crt.	X ₁	Y ₁	Z ₁	X ₃	Y ₃	Z ₃	Count vector	Theta	Count Theta	Phi	Count Phi
	<i>m</i>	<i>m</i>	<i>m</i>	<i>m</i>	<i>m</i>	<i>m</i>	<i>N</i>	degrees	<i>N</i>	degrees	<i>N</i>
1	0.36	0.24	0.51	0.36	-0.08	-0.51	243	180	701 371	162.41523	555 091
2	-0.4	0.24	0.51	-0.4	-0.08	-0.51	233	180	701 371	162.41523	555 091
3	0.28	-0.44	0.51	0.28	-0.12	-0.51	232	180	701 371	162.41523	555 091
–	–	–	–	–	–	–	–	–	–	–	–
72 862	-0.44	0.48	0.51	0.52	-0.4	-0.51	33	-42.51045	39	128.18348	44
72 863	-0.44	0.4	0.51	0.52	-0.48	-0.51	6	-42.51045	39	128.18348	44
72 864	-0.44	-0.4	0.51	0.52	0.48	-0.51	5	42.51045	5	128.18348	44

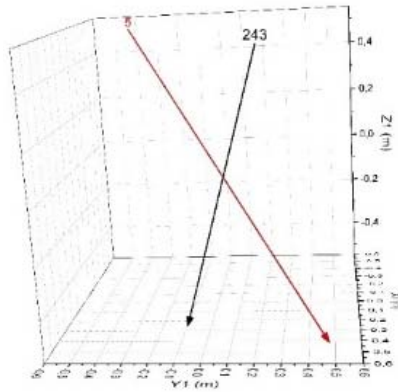


Fig. 16 – Statistical vector (a) – for a measuring uncertainty of (+/-) 0.04 m.

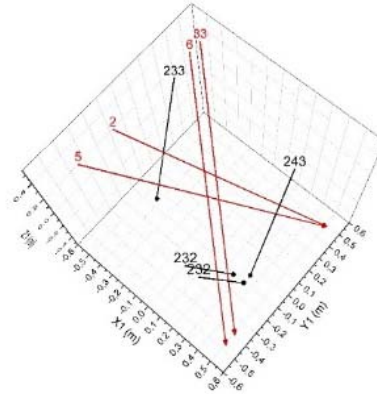


Fig. 17 – Statistical vector (b) – for a measuring uncertainty of (+/-) 0.04 m.

Table 3

(Truncated) table containing data for the statistical analysis of incident vectors with approximation of 0.08 m

Nr. Crt.	X1	Y1	Z1	X3	Y3	Z3	Count vector	Theta	Count Theta	Phi	Count Phi
	m	m	m	m	m	m	N	degrees	N	degrees	N
1	0.28	0.12	0.51	0.28	-0.28	-0.51	587	180	1.68405E6	158.0136	1.38766E6
2	0.36	0.28	0.51	0.36	-0.12	-0.51	513	180	1.68405E6	158.0136	1.38766E6
3	0.36	0.12	0.51	0.36	-0.28	-0.51	508	180	1.68405E6	158.0136	1.38766E6
4	-0.2	0.12	0.51	-0.2	-0.28	-0.51	503	180	1.68405E6	158.0136	1.38766E6
–	–	–	–	–	–	–	–	–	–	–	–
85 232	0.44	-0.44	0.51	-0.52	0.52	-0.51	9	-45	568 484	126.8699	51
85 233	-0.4	0.44	0.51	0.56	-0.52	-0.51	5	45	561 634	126.8699	51
85 234	-0.44	-0.44	0.51	0.52	0.52	-0.51	15	45	561 634	126.8699	51
85 235	-0.4	-0.44	0.51	0.56	0.52	-0.51	8	45	561 634	126.8699	51

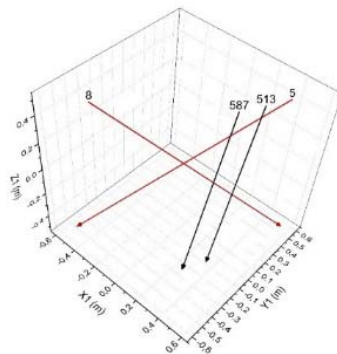


Fig. 18 – Statistical vector (a) – for a measuring uncertainty of (+/-) 0.08 m.

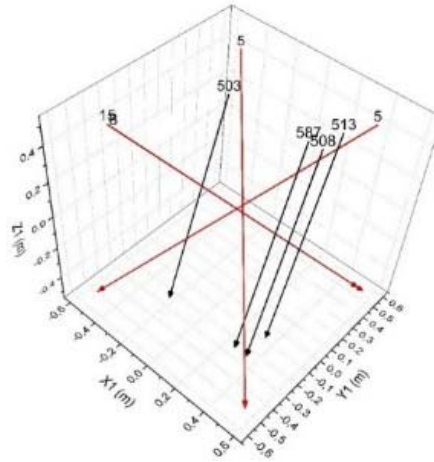


Fig. 19 – Statistical vector (b) – for a measuring uncertainty of (+/-) 0.08 m.

4. CONCLUSIONS

The photographs below show the placement of the lab in which the detector is found.

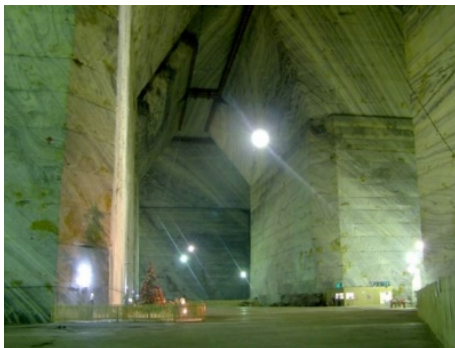


Fig. 20 – Placement of the subterranean lab.

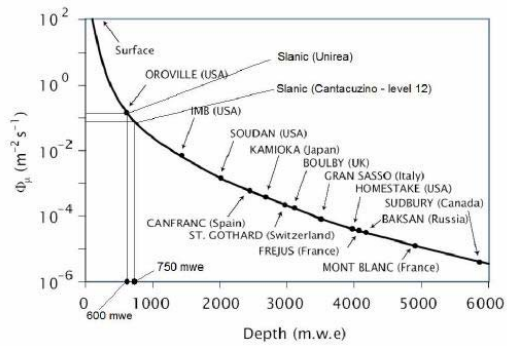


Fig. 21 – Underground muon flux.

- A – muon lab
- B – high resolution gamma spectroscopy
- C – office
- D – low background dosimetry [9]

From the set of graphs presented previously, we can draw the following conclusions:

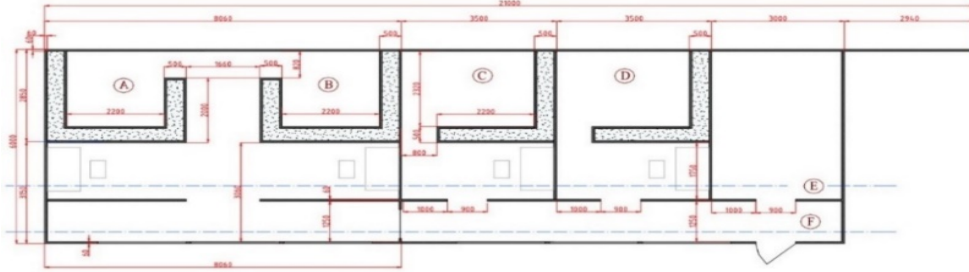


Fig. 22 – Schematic lab.

Location	Depth (from surface)	Muon flux ($\text{m}^{-2} \text{s}^{-1}$)	mwe depth
Unirea mine	- 208 m	0.18 ± 0.01	610 ± 7
Cntacuzino mine – Level 8	- 188 m	0.19 ± 0.02	601 ± 9
Cntacuzino mine – Level 12	- 210 m	0.09 ± 0.01	790 ± 13

- The optimum error applicable to these geometries (see Figs. 9, 18 and 19) is 0.08 m.
- We observe that we have two preferred spatial directions for which the number of muons passing simultaneously through the three detection planes can be classified as a minimum and maximum. These directions are given by the quantity of the substance, rock found in the path of the muon radiation, and which has an attenuation role.
- From the statistical representations above we can also evaluate the flux variation of the muonic radiation, not only its direction but also the method could implicitly, after some calibration, give more information on the quality as well as the quantity of the material through which the muons pass.

These facts allow us to appreciate the way in which the routines of the software application treat the physical phenomenon with the purpose of highlighting with high accuracy certain preferred directions (in three dimensions) of the muon flux. Through comparative treatment of the three calculation options, for 0.04 m, 0.08 m and 0.12 m deviation in detection, deviation due to the large size of the detection cell compared to the way the incident muon particle is detected, we can calibrate our results for the potential other detection missions in different working geometries.

In this case, very clearly regarding how the muon flux varies, we can test the application built based on algorithms that take into consideration the nature and geometry of the detector. Once we confirmed the procedure, we can commence the

actual research of zones with homogeneity variation in the rock, the walls of a mine cavern or other objectives to which it is suitable. This technique can be used equally as well in real-time mode, in the detection of the variation of dense or less dense material in border places, of nondestructive research at minimal cost, using muonic radiation. The method presented can be used with excellent results in building a muon detection system underground to investigate some fundamental problems in Astroparticle physics, the possibility of detecting unknown cavities using subterranean measurements of muons [10].

The method has been tested for two sets of measurements, and for multiple sets of errors in measurement of the number of coincidences, errors generated by the large size of the detector cell. The possibility of real-time results extraction renders this method also useful in the NEMO project in the Constanta Port.

Through this method, information can be collected from a network of detectors fitted in different places, which send (*via* an internet connection), synchronized with a time base, the detection collated in an online database. The synchronization of detector time bases can be done simultaneously before the installation at specific coordinates or online due to the internet connection that we need to have, as the data is collected through the web, or we can perform a calibration (time correction) offline, in the database. Then, using the coincidences algorithm described in this paper, we can extract in real-time quantitative and qualitative information about the terrestrial structure we are studying.

SUPPLEMENTARY MATERIALS

The following are available online:

- Databases structure at https://liviunita.ro/download/dumps_fitm.zip;
- Full article with programing code at https://liviunita.ro/download/full_article.docx.zip;
- Installation kit for desktop windows application at https://liviunita.ro/fitm_kit.zip.

For user access please contact at liviunita.ro@gmail.com. Data supporting reported results can be found at <https://liviunita.ro/fitm>.

Acknowledgements. I would like to express my gratitude to the scientific coordinator, Prof. Univ. Dr. Alexandru JIPA, director of the Department of Matter Structure, Atmospheric and Earth Physics, Astrophysics at the Faculty of Physics of the University of Bucharest. I would like to thank him for his continued support of this doctoral dissertation, for his patience, dedication, and professionalism.

REFERENCES

1. F. Sauli, *GEM: A new concept for electron amplification in gas detectors*, Nucl. Instrum. Meth., **A386**, 531–534 (1997).
2. Y. Giomataris, P. Rebourgeard, J. Robert, G. Charpak, *Micromegas: A high granularity position sensitive gaseous detector for high particle flux environments*, Nucl. Instrum. Meth. **A376**, 29–35 (1996).
3. R.M. Mărgineanu, A.M. Apostu, O.G. Dului, S. Bercea, C.M. Gomoiu, C.I. Cristache, *External dose rate in Unirea salt mine, Slanic-Prahova, Romania*, Applied Radiation and Isotopes **67**, 759–781 (2009).
4. A. Gezerlis, *Numerical Methods in Physics with Python*, Cambridge University Press, 2020, pp. 311–387.
5. J.H. Mathews, *Numerical Methods: for Mathematics, Science and Engineering*, London, Prentice-Hall International, 1992.
6. <https://www.vfphelp.com/help/>
7. The Pierre Auger Collaboration, *Calibration of the underground muon detector of the Pierre Auger Observatory*, 7-12, JINST 16 P04003 (2021).
8. <https://dev.mysql.com/doc/refman/8.0/en/help.html>
9. B. Mitrică, R. Mărgineanu, S. Stoica, M. Petcu, I. Brancus, Al. Jipa, I. Lazanu, O. Sima, A. Haungs, H. Rebel, M. Petre, G. Toma, A. Saftoiu, D. Stanca, A. Apostu, C. Gomoiu, *A mobile detector for measurements of the atmospheric muon flux in underground sites*, Nuclear Instruments and Methods in Physics Research **A 654** (2011).
10. F. Collamati, C. Curatolo, D. Lucchesi, A. Mereghetti, N. Mokhov, M. Palmere, P. Sala, *Advanced assessment of beam-induced background at a muon collider*, JINST 16 P11009, 11–14 (2021).